Journal of Power Sources 270 (2014) 151–157

Contents lists available at ScienceDirect

Journal of Power Sources

journal homepage: www.elsevier.com/locate/jpowsour

A method for state of energy estimation of lithium-ion batteries at dynamic currents and temperatures

Xingtao Liu, Ji Wu, Chenbin Zhang, Zonghai Chen*

Department of Automation, University of Science and Technology of China, Hefei 230027, PR China

HIGHLIGHTS

- The state of energy (SOE) is introduced to replace the SOC to determine the residual energy of the battery.
- The energy loss on the internal resistance, electrochemical reactions and decrease of OCV is considered in SOE estimation.
- Temperature and current influence are considered to improve the robustness of SOE estimation.
- The proposed BPNN method is validated under dynamic temperature and current conditions.

ARTICLE INFO

Article history:
Received 15 June 2014
Received in revised form
15 July 2014
Accepted 16 July 2014
Available online 24 July 2014

Keywords:
Lithium-ion battery
State of energy
Neural network
Dynamic current
Temperature

ABSTRACT

The state of energy (SOE) of Li-ion batteries is a critical index for energy optimization and management. In the applied battery system, the fact that the discharge current and the temperature change due to the dynamic load will result in errors in the estimation of the residual energy for the battery. To address this issue, a new method based on the Back-Propagation Neural Network (BPNN) is presented for the SOE estimation. In the proposed approach, in order to take into account the energy loss on the internal resistance, the electrochemical reactions and the decrease of the open-circuit voltage (OCV), the SOE is introduced to replace the state of charge (SOC) to describe the residual energy of the battery. Additionally, the discharge current and temperature are taken as the training inputs of the BPNN to overcome their interference on the SOE estimation. The simulation experiments on $LiFePO_4$ batteries indicate that the proposed method based on the BPNN can estimate the SOE much more reliably and accurately.

1. Introduction

With the improvement of the energy density and the safety performance, Li-ion batteries are widely used in the renewable energy vehicles and energy storage systems, such as electric vehicles, wind power systems, solar power systems, micro-grid and so on. The SOE of the battery [1], which provides the essential basis of energy deployment, load balancing, and security of electricity for the complex energy systems, is a key parameter in the battery system.

Traditionally, the residual energy of the battery is represented by the estimation of the SOC. In recent years, many studies on the SOC estimation can be found in the literature, with the primary methods being the current integral method [2], the electrical model based method [3–7] and the neural network model method [8–10].

The current integral method obtains the SOC estimation through the accumulation of the battery current [2]. The method is easy to implement; however it is an open-loop estimation so that its estimation accuracy becomes poor due to the accumulated error caused by the current measurement noise [7]. As to the electrical model based method, both electrochemical models and equivalent circuit models are established to capture the relationship between the SOC and the OCV of the battery. Then, the Kalman filter methods or the particle filter methods are applied for the SOC estimation based on these battery models. The Kalman filter and particle filter methods are closed-loop, and many algorithms such as extended Kalman filter [5,6,11], unscented Kalman filter [12,13] and unscented particle filter [3,5] are used in the SOC estimation. These methods take the SOC as a state variable, so they can solve the accumulated error of the current integral method by updating the SOC on the basis of the difference between the measured and the prediction value of the terminal voltage. The neural network model methods can describe the dynamic and nonlinear behavior of the battery by means of the multilayer neural networks, and thus

* Corresponding author. Tel.: +86 055163606104.
E-mail address: chenzh@ustc.edu.cn (Z. Chen).

http://dx.doi.org/10.1016/j.jpowsour.2014.07.107
0378-7753/

it could be used to estimate the SOC for Li-ion batteries [8–10]. Some works develop the data-fusion method [14] and the discrete Wavelet method [15,16] for SOC estimation. These approaches have been widely used in the SOC estimation of Li-ion batteries, and most of them have achieved acceptable results.

Nevertheless, with the increasingly widespread application of Li-ion batteries, the functional demand of battery management system appears a more sophisticated and complex trend. Therefore, the disadvantages of using the estimated SOC to represent the battery residual energy become more prominent. Firstly, the SOE is different from the SOC for Li-ion batteries. The SOC defines the ratio of the residual active material to the total original active material inside a Li-ion battery. In this sense, the SOC indicates only the capacity state rather than the energy state on which the battery application conditions is dependent. For a more detailed management of the battery, the discharge efficiency and the residual energy are necessary. There are no more energy information can be got from the estimated SOC since the SOC is only a percentage of the battery capacity. Some works have considered the residual available capacity instead of the SOC to determine the residual energy of the battery [17–20]. Secondly, although there is a positive correlation between the SOE and the SOC, they have no explicit quantitative relationship. The SOC decreases linearly with the discharge current, but the battery energy is the product of the capacity and the OCV of the battery. There are differences between the SOC and the SOE because the energy loss on the internal resistance, the electrochemical reactions and the decrease of the OCV are not considered in the SOC estimation [3–5,21–24]. Thirdly, in the actual battery system, where the discharge current and the temperature usually changes dramatically due to the dynamic load, the performance of the battery becomes poor [25–27]. For SOC estimation, the temperature effect has been considered to build a more accurate battery model [13,28,29]. Xing et al. [28] develop an offline OCV–SOC-temperature table to describe the temperature effect, and pattern recognition based on the Hamming network is presented to check the temperature [29]. However, as to the relation between the SOE and the temperature, it is not adequately addressed in the recent literature. At the same SOC, the SOE may change on account of the fact that the discharge efficiency is dependent on the discharge current and temperature. Thus, it is necessary to carry on a more comprehensive analysis on the effect of the discharge current and temperature for getting a more accurate SOE estimation.

In this paper, to determine the energy loss on the internal resistance, the electrochemical reactions and the decrease of the OCV, the SOE instead of the SOC is introduced to represent the residual energy of Li-ion batteries, and a BPNN method is proposed to improve the SOE estimation at dynamic currents and temperatures. In Section 2, we give a clear definition of the SOE for Li-ion batteries. Battery tests with various currents at different temperatures are carried out to analyze their effect on the SOE in Section 3. In Section 4, a BPNN battery model is established to take into account the effect of the OCV, discharge current and temperature. And then, parameters of the BPNN battery model are identified by the experimental data of $LiFePO_4$ batteries. In Section 5, simulations based on the BPNN algorithm are used to verify the accuracy of the estimation of the battery SOE.

2. SOE

The SOE provides the information of the remaining available energy of Li-ion batteries [30,31], so it is a critical parameter for energy optimization and management for the battery system. In this paper, the SOE is defined as:

$$SOE(t) = E_c - E_d(t) \quad (1)$$

where $SOE(t)$ is the remaining energy of the battery at time t, E_c is the total energy of the battery and $E_d(t)$ is the discharged energy of the battery until time t. Generally, the SOE reaches its maximum after it is fully charged, and the SOE is zero when the battery is discharged to its low cutoff voltage.

The study of Li-ion batteries indicates that the energy, which is consumed during the discharge process, is mainly composed of the output electric energy, the energy consumed on the internal resistance heating and the energy consumed on the electrochemical reactions. The output electric energy is used to meet the load, and it is usually expressed by the SOC in previous studies. The internal resistance will heat the battery during the discharge process, so it expends the battery energy. The electrochemical reactions inside the battery also cause the energy consumption.

The available energy of Li-ion batteries changes with the battery temperature. Specifically, the available energy decreases significantly at low temperatures. Under high discharge currents, a Li-ion battery may demonstrate empty conditions via the low cutoff voltage. However, the battery still has energy that may be utilized at lower discharge currents. This characteristic can bring great difficulties to the estimation accuracy of the SOE.

3. Experiments

3.1. Test bench

In order to acquire experimental data of Li-ion batteries, a test bench is built, as shown in Fig. 1. The test bench is composed of a battery test system NEWARE BTS4000, a battery management system (BMS), a CAN communication unit, a host computer for online experiment control and a programmable temperature chamber. The NEWWARE BTS4000 is used to load the battery with a maximum voltage of 5 V and a maximum current of 100 A, and its voltage and current measurement accuracy is ±0.1%. The experimental data such as current, voltage, temperature, accumulative ampere-hours (Ah) and Watt-hours (Wh) are measured by the NEWWARE BTS4000 and recorded by the host computer. The BMS

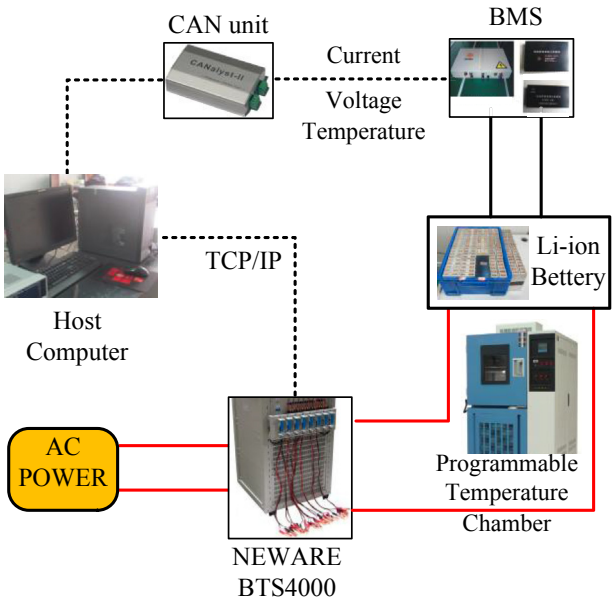

Fig. 1. Configuration of the battery test bench.

Table 1
Parameters of a $LiFePO_4$ cell.

Parameter	Rated capacity	Low voltage cutoff	Upper voltage limit	Operating temperature
Value	9 Ah	2.0 V	3.65 V	−20 °C–60 °C

performs the functions of battery protection and transmits the data of the fault information to the host computer through the CAN communication unit. The programmable temperature chamber provides manageable temperatures for the battery. The test is carried out with $LiFePO_4$ batteries with a rated capacity of 9 Ah (produced by HeFei GuoXuan High-Tech Power Energy CO., Ltd. of China). The parameters of the battery are given in Table 1.

3.2. OCV test

After the battery standing for a long period, the terminal voltage will achieve the true OCV value. In order to acquire data to identify the OCV, a test was performed on $LiFePO_4$ batteries. The test procedure is designed as follows: the battery is first discharged by a 10% of the nominal capacity from fully charged state at the preset current. Afterward it is left in open-circuit state and the OCV is monitored simultaneously. The measured OCV is considered to reach to the equilibrium potential after three hours until the change of the OCV is statistically insignificant and the battery is assumed to reach to a steady state. The battery is continuously discharged by a further 10% of the nominal capacity at the same current. The above procedure is performed repeatedly to obtain the OCV data until the battery reaches the low cutoff voltage in Table 1. The discharge current rate is set to 0.5C, 1C, 3C and 5C, respectively. Then the average under these currents is taken as the result. The OCV data are plotted in Fig. 2.

According to Fig. 2, the OCV curve decreases with the discharge rapidly, especially at the beginning and the end of the discharge process. In detail, when the SOC decreases from 100% to 0%, the OCV also decreases from 3.433 V to 2.814 V. Because the battery energy is the product of the OCV and the capacity, at the same interval of the SOC, the discharged energy of the battery is not a constant. Furthermore, in order to investigate the differences between the discharged capacity and the discharged energy, we calculate the discharged energy at a 10% interval of the SOC from 100% to 0%. The results are shown in Fig. 3.

Fig. 3 describes the change of the discharged energy with SOC, and the *Y*-axis represents the discharged energy. In Fig. 3, the discharged energy appears a decreasing trend with the decreasing SOC. When the SOC decreases from 100% to 90%, the discharged energy of the battery is 2.945 Wh. When the SOC decreases from 10% to 0%, the discharged energy is only 2.215 Wh. The discharged energy of the battery presents a change at different SOC. A battery system is usually composed of hundreds or thousands of cells through series and parallel electrical connections, so the differences shown in Fig. 3 will be larger in actual operation. Thus, the SOC cannot capture the energy behavior of the battery accurately according to these statistical data analysis.

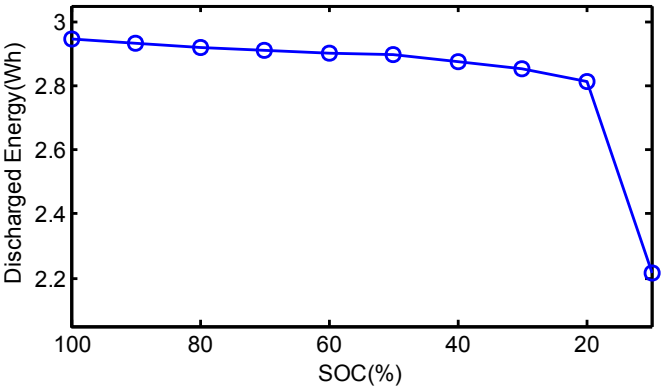

Fig. 3. The discharged energy at different SOC.

3.3. Battery test with various currents at different temperatures

In order to investigate the discharged energy of the battery with various currents at different temperatures, we load the battery with the discharge current 0.5C, 1C, 2C, 3C, 4C, 5C, 6C and 7C at temperature 0 °C, 10 °C, 25 °C and 45 °C, respectively. First, the battery is left in the open-circuit state at room temperature for three hours until the OCV reaches a steady state. Then, it is fully charged with a constant current of 0.5C at room temperature. And then, the battery is left in the programmable temperature chamber at the constant preset temperature for another three hours until the change of the battery voltage is negligible and the battery is considered to reach a steady state. After that, the battery is discharged with the constant preset current at the same temperature until the battery voltage reaches to the low cutoff value. The procedure is carried out repeatedly. We plot the discharged energy of the battery with various currents at different temperatures in Fig. 4.

When the temperature is 25 °C, the discharged energy of the battery is 29.469 Wh at 0.5C discharge rate, while it is 25.902 Wh at 7C discharge rate. We can found that the discharged energy has a

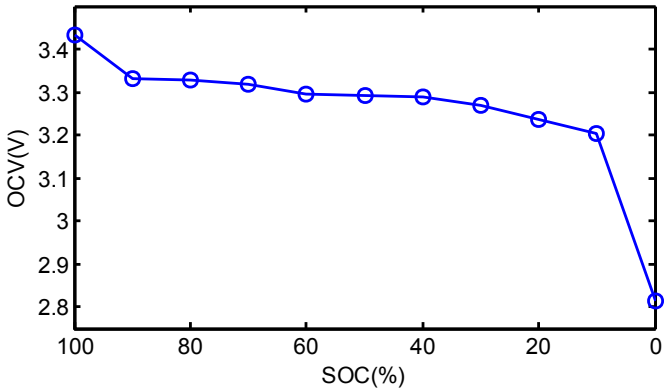

Fig. 2. OCV curve of the battery.

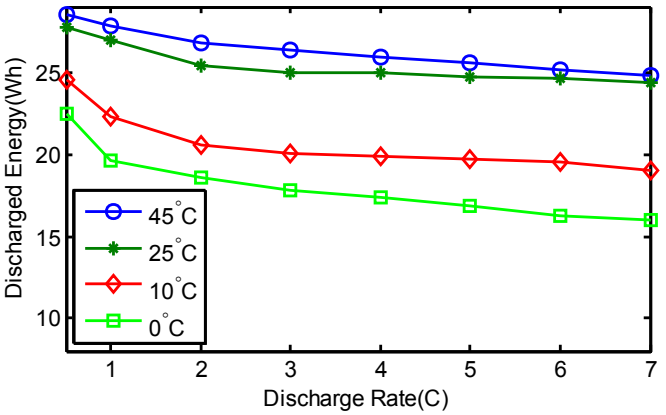

Fig. 4. The discharged energy with various currents at different temperatures.

decreasing trend with the increasing discharge rate at the same temperature. As to the temperature, when the discharge rate is 2C, the discharged energy of the battery are 19.731 Wh, 21.822 Wh, 26.978 Wh and 28.414 Wh at temperatures of 0 °C, 10 °C, 25 °C and 45 °C, respectively. The discharged energy presents a significant increase with the rising temperature. The discharged energy of the battery is greatly related on the discharge efficiency which varies with the discharge currents and temperatures. Therefore, there is a need to study a method to realize an accurate SOE estimation under various currents and temperatures conditions.

4. Battery modeling using BPNN for SOE estimation

The charge–discharge process of a Li-ion battery is full of complex electrochemical reactions, and there are no explicit quantitative formulas to describe the relationship between the SOE and battery parameters (voltage, current and temperature) owning to the complex mechanism and multitudinous parameters inside the battery. The fact that the SOE is dependent on the dynamic load makes more sense to investigate an accurate battery model for the SOE estimation. As a highly nonlinear black box system, the BPNN does not need accurate relationship formulas to describe the dynamic behavior of the battery because the relationship can be automatically generated when the network was trained with the history data. Aiming at the effect of the current and temperature on the SOE estimation, a BPNN method for the SOE estimation is proposed in this paper.

4.1. The structure of the BPNN

The BPNN can perform the nonlinear function approximation in accordance with the design accuracy requirements. According to the requirements of the SOE estimation for Li-ion batteries, the BPNN is consisted of 3 layers-the input layer, the hidden layer and the output layer. The experimental results in Section 3 indicate that the SOE is related to the OCV, the discharge current and the temperature. As a result, in the input layer, the battery terminal voltage, the current and the temperature ([*V*, *I*, *T*]) are taken as the input parameters. As the terminal port of the BPNN battery model, the output layer is the estimated SOE. The structure of the BPNN for the SOE estimation is shown in Fig. 5.

The input vector of the input layer is $\mathbf{X} = (V, I, T)^T$, the output vector of the hidden layer is $\mathbf{O} = (o_1, o_2, \ldots, o_m)^T$, the weight matrix of the neurons in the hidden layer is $\mathbf{Q} = (q_{11}, \ldots, q_{ij}, \ldots, q_{3m})^T$; the output vector of the output layer is $\mathbf{Y} = SOE$, the weight matrix of the neurons in the output layer is $\mathbf{W} = (w_1, \ldots, w_i, \ldots, w_m)^T$. According to the training results of the BPNN, the number of the neurons in the hidden layer m is 12. Set the threshold value of the neurons in the hidden layer as $\boldsymbol{\theta}$, so the mathematical equations of the hidden layer can be expressed as follows.

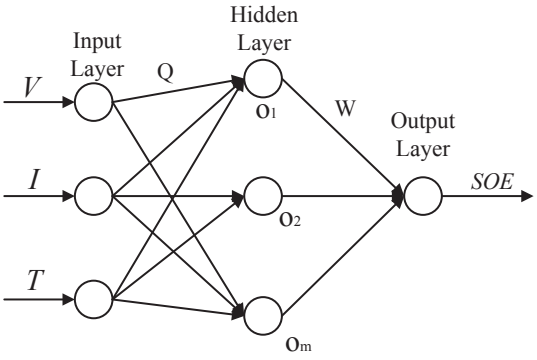

Fig. 5. The structure of the BPNN.

$$o_i = f\left(\sum_{j=1}^{3} q_{ji}x_j + \theta_i\right) \quad i = 1, 2, \ldots, m \tag{2}$$

Set the threshold value of the neurons in the output layer as λ, so the mathematical equations of the output layer is:

$$SOE = g\left(\sum_{j=0}^{m} w_j o_j + \lambda\right) \tag{3}$$

$f(\cdot)$ and $g(\cdot)$ represent the activation functions of the hidden layer and the output layer, respectively.

4.2. SOE estimation based on the BPNN

When the BPNN battery model is used to estimate the SOE at the first time, a number of actual data samples [*V*, *I*, *T*, SOE] are selected to train the BPNN primarily. The training process of the BPNN is carried out as follows: the learning samples including the data of battery voltage, current and temperature enter the network from the input layer firstly. The output value of the SOE is got from the output layer after the calculations by the BPNN. Then, the differences between the output value and the actual value of the SOE are transmitted from back to front in the BPNN. On the basis of the differences, the network weight matrixes are updated by the learning algorithm until the output error of the network achieves the target termination condition. The Levenberg–Marquardt back-propagation algorithm, which is an efficient implementation of a quasi-Newton method to estimate the network parameters, is used to train the BPNN. When the weight matrixes were determined through the training process, the BPNN could be applied for the SOE estimation.

$$SOE = g\left(\mathbf{W}^{\mathrm{T}} \cdot f\left(\mathbf{Q}^T\mathbf{X} + \boldsymbol{\theta}\right) + \lambda\right) \tag{4}$$

where $\boldsymbol{W}$ represents the weight matrix of the neurons in the output layer, $\mathbf{Q}$ represents the weight matrix of the neurons in the hidden layer, $\mathbf{X}$ represents the input vector of the input layer, $\boldsymbol{\theta}$ represents the threshold value of the neurons in the hidden layer and λ represents the threshold value of the neurons in the output layer.

An enormous amount of information about the energy loss and the relationship between the residual energy and the dynamic load (discharge current and temperature) are implicit in the experimental training data. During the experiments, the battery voltage, current, temperature and experimental time are measured and recorded as the training data. Due to the self-learning capability of the BPNN, an accurate SOE will be obtained as long as the training data is substantial. The determined weight matrixes can be written in the EEPROM of battery management system, and then the trained BPNN will be able to apply in the actual operation of electric vehicles.

4.3. Parameters identification of the BPNN

In order to acquire battery data to train the BPNN model and identity the model parameters, we load the $LiFePO_4$ batteries with various discharge currents at different temperatures. The experiments are carried out on the battery test bench in Subsection 3.1. The charge and discharge process of the battery is performed by the NEWWARE BTS4000 with a designed operation mode, and the temperature is controlled by the programmable temperature chamber.

Firstly, set the sample period of the NEWWARE BTS4000 to be 1 s and start the data acquisition module in the host computer to collect the battery voltage, current and temperature automatically.

Secondly, load the battery at different temperatures with a static current and record the experimental data. The battery is discharged with the current 0.5C, 1C, 2C, 3C, 4C, 5C, 6C and 7C at temperature 0 °C, 10 °C, 25 °C and 45 °C, respectively. When the battery is discharged to the low cutoff voltage in Table 1, stop the discharge process. After the battery is fully discharged, it is left at room temperature (25 °C) for three hours, and then it is charged with the charge current, which is the same with the discharge current value. During the charge process, the battery is charged with the constant preset charge current until the battery reaches the upper limit voltage in Table 1, then the NEWWARE BTS4000 keeps the charge voltage unchanged and gradually reduces the charge current. Stop the charge process when the value of the charge current reaches zero.

Thirdly, load the battery under dynamic conditions. The battery is operated at the dynamic discharge current conditions shown in Fig. 6 and a constant rate of temperature rise from 0 °C to 60 °C. The total available discharged energy could be obtained by integrating the current curve and the voltage curve of the whole process.

Finally, the BPNN model is trained on the basis of the differences between the output value and the actual value of the SOE. The target error of the BPNN training is given by the mean square error (MSE) as follows:

$$E_{\text{mse}} = \frac{1}{l}\sum_{p=1}^{l}(SOE_{\text{r}}(p) - SOE_{\text{e}}(p))^2 \tag{5}$$

where E_{mse} represents the MSE between the estimated and the actual SOE, l represents the number of the training data, $SOE_{\text{r}}(p)$ represents the actual SOE of the training data group p and $SOE_{\text{e}}(p)$ represents the estimated SOE by the BPNN method.

5. Simulation experiment and discussion

In this section, validation experiments are performed with the $LiFePO_4$ batteries with a rated capacity of 9 Ah to verify the performance of the SOE estimation by the BPNN method with various discharge currents at different temperatures.

As analyzed in Section 4, we propose a SOE estimation approach based on the BPNN, in which the effect of the temperature is considered. In order to verify the proposed method at different temperatures, the battery is discharged with a constant 0.5C rate at temperature 15 °C, and the comparison results of the estimated and

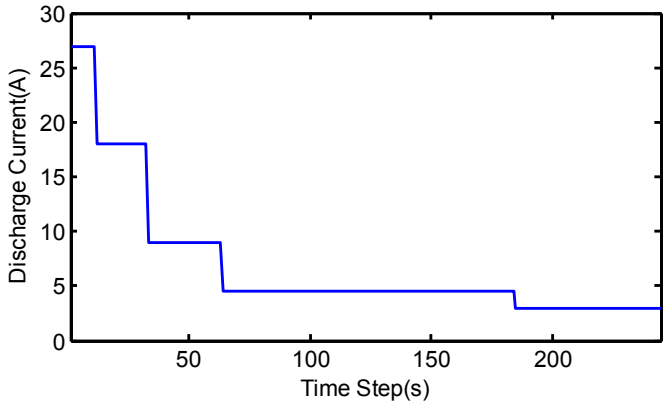

Fig. 6. Dynamic current conditions.

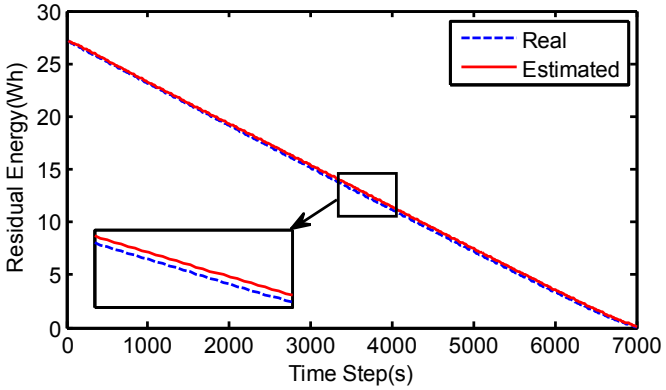

Fig. 7. SOE estimation results of the BPNN at 15 °C.

the actual SOE are plotted in Fig. 7. As shown in Fig. 7, the general shape of the estimated SOE and that of the true experimental value are almost the same.

The temperature usually changes dramatically in the battery system during the actual operation. As the battery is discharged at a constant rate of the temperature rise from 5 °C to 60 °C, Fig. 8 shows the comparison results of the estimated and the actual SOE when a constant 0.5C rate fully discharge is run. Fig. 8(a) shows the change of the battery temperature, and Fig. 8(b) shows the estimation results of the SOE by the BPNN method. The BPNN method tries to determine the effect of the temperature and can provide an accurate SOE estimation at dynamic temperature conditions.

Furthermore, during the actual battery working conditions, the discharge current also dynamically changes due to that the power requirement of the load varies with time. According to the

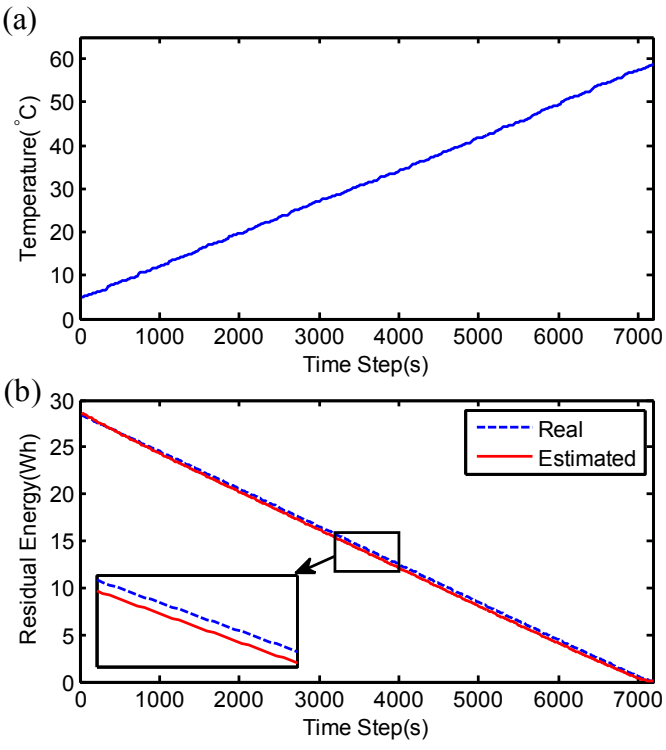

Fig. 8. SOE estimation results at dynamic temperatures: (a) Dynamic temperature conditions. (b) The comparison of the estimated and the actual SOE.

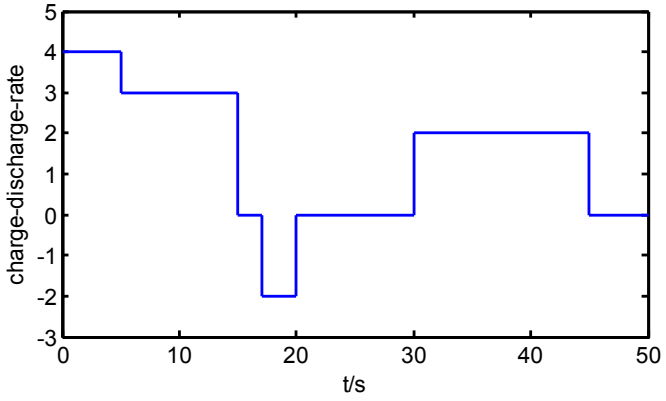

Fig. 9. Current of the simulation operation conditions.

corresponding BMS test procedures in Ref. [32], the battery is loaded repetitively at the current of the simulation operation conditions shown in Fig. 9 until the battery is discharged to the low cutoff voltage. The temperature of the battery post pillar is measured with thermocouples, and the temperature rises from 20 °C to 35 °C freely. The aim is to investigate the effectiveness of the BPNN method under dynamic current and temperature conditions.

Fig. 10(a) shows the estimated SOE by the BPNN method when the battery is loaded under the current conditions in Fig. 9. In Fig. 10(a), the root-mean-square error between the actual SOE and the estimated SOE is 1.314, and the BPNN algorithm still gives an acceptable result under dynamic conditions. Additionally, in order to validate the advantage of the SOE over the SOC, we compare the real SOE, the estimated SOE, the real SOC and the estimated SOC ratio, and give the results in Fig. 10(b) and Table 2. The actual SOC value is calculated with the measured current curve after the battery has suffered the discharge test, and the estimated SOC is obtained by the unscented Kalman filter (UKF) method. As shown in Fig. 10(b), both the real SOC and the estimated SOC appear a deviation from the true SOE curve, especially at the latter part of the discharge process. Because the energy loss on the internal resistance, the electrochemical reactions and the decrease of the OCV is considered in the SOE estimation, the accuracy of the SOE estimation appears an improvement over the SOC in capturing the energy behavior of the battery. The battery system in EVs is usually composed of a large number of cells, so the differences between the SOE and the SOC shown in Fig. 10(b) become more significant.

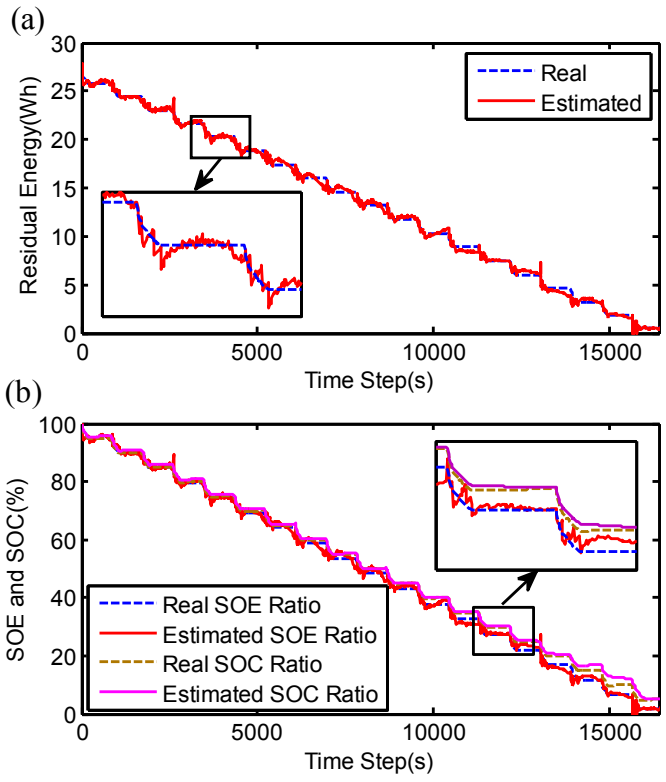

Fig. 10. SOE estimation results at dynamic currents and temperatures: (a) The comparison of the estimated and the actual SOE. (b) The comparison of the SOC and the SOE.

Table 2
The numerical results of the estimated SOE and SOC ratio.

Total value	Method	RMSE[a]
27.177 Wh	Estimated SOE by BPNN	0.012
8.725 Ah	Real SOC	0.019
8.725 Ah	Estimated SOC by UKF	0.027

[a] RMSE = root-mean-square error.

The voltage acquisition circuit in the BMS may inevitably produce measurement noise during the actual operation. Assuming that the measured battery voltage contains a measurement error (set a 5 mV voltage error), Fig. 11 presents the estimated SOE by the BPNN method. The estimated SOE curve is close to the true value, so the proposed method can suppress the interference of the voltage measurement noise to get an accurate SOE estimation. In the actual data acquisition circuit, multiple measurements could be applied to reduce the measurement error.

Based on the above results and analysis, we can conclude that the BPNN method can achieve an accurate SOE estimation at dynamic current and temperature conditions. This is mainly because the energy loss, the effect of the discharge current and the temperature are considered in the proposed method.

6. Conclusions

With the continuous advancement of the battery technology, the applications of Li-ion batteries are becoming more widespread. In the actual applications, the fact that the current and temperature changes significantly during the discharge process puts forward a great challenge to the energy management of the power source. A new method based on the BPNN is presented for the SOE estimation in this paper. The SOE, instead of the SOC, is introduced to

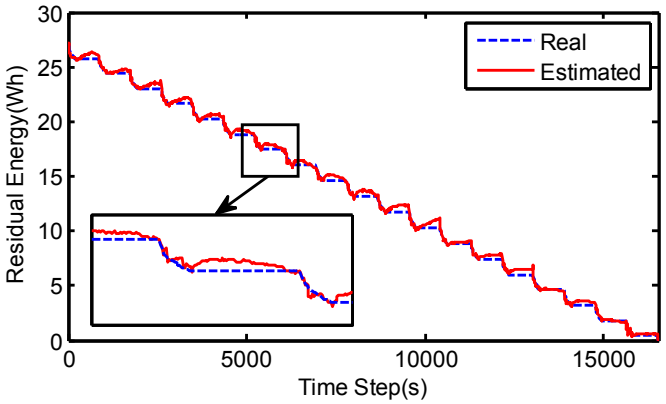

Fig. 11. The SOE estimation with a voltage error.

describe the energy state of the battery. In the SOE estimation, the energy loss on the internal resistance, the electrochemical reactions and the decrease of the OCV is considered more comprehensively. To suppress the interference caused by dynamic currents and temperatures, a BPNN battery model is proposed for the SOE estimation and the battery voltage, current and temperature are taken as the training inputs. Finally, the good accuracy of the simulation based on the actual experimental data verifies the presented approach. Thus, it provides a proper solution for the SOE estimation under dynamic application conditions. To reduce the hardware cost, the complexity of the BPNN method needs to be further addressed in future studies.

Acknowledgments

This work was supported by the National Natural Science Foundation of China (Grant No. 61375079).

References

[1] K. Mamadou, A. Delaille, E. Lemaire-Potteau, Y. Bultel, ECS Trans. 25 (2010) 105–112.
[2] Kong Soon Ng, Chin-Sien Mooa, Yi-Ping Chen, Yao-Ching Hsieh, Appl. Energy 86 (2009) 1506–1511.
[3] Y. He, X. Liu, C. Zhang, Z. Chen, Appl. Energy 101 (2013) 808–814.
[4] G. Plett, J. Power Sources 134 (2004) 262–276.
[5] L. Zhong, C. Zhang, Y. He, Z. Chen, Appl. Energy 113 (2014) 558–564.
[6] G. Plett, J. Power Sources 134 (2004) 277–292.
[7] X. Liu, X. Liu, Y. He, Z. Chen, Kongzhi Yu Juece/Control Decis. 25 (2010) 445–448.
[8] L. Kang, X. Zhao, J. Ma, Appl. Energy 121 (2014) 20–27.
[9] L. Xu, J. Wang, Q. Chen, Energy Convers. Manag. 53 (2012) 33–39.
[10] J. Bi, S. Shao, W. Guan, L. Wang, Chin. Phys. B 21 (2012).
[11] R. Xiong, F. Sun, Z. Chen, H. He, J. Power Sources 113 (2014) 463–476.
[12] F. Sun, X. Hu, Y. Zou, S. Li, Energy 36 (2012) 3531–3540.
[13] Z. He, M. Gao, C. Wang, L. Wang, Y. Liu, Energies 6 (2013) 4134–4151.
[14] J. Yan, G. Xu, H. Qian, Y. Xu, Energies 3 (2010) 1654–1672.
[15] J. Kim, W. Kim, J. Park, C. Chun, B. Cho, in: IEEE Energy Conversion Congress and Exposition, 2012, pp. 3187–3192.
[16] J. Kim, C. Chun, B. Cho, in: 280th Annual IEEE Applied Power Electronics Conference and Exposition, 2013, pp. 2720–2725.
[17] W. Shen, Energy Convers. Manag. 48 (2007) 433–442.
[18] Y. Zheng, L. Lu, X. Han, J. Li, M. Ouyang, J. Power Sources 226 (2013) 33–41.
[19] W. Waag, D. Sauer, Appl. Energy 111 (2013) 416–427.
[20] A. Hausmann, C. Depcik, J. Power Sources 235 (2013) 148–158.
[21] J. Xun, R. Liu, K. Jiao, J. Power Sources 233 (2013) 47–61.
[22] B. Wu, V. Yufit, M. Marinescu, G. Offer, R. Martinez-Botas, N. Brandon, J. Power Sources 243 (2013) 544–554.
[23] H. Sun, X. Wan, B. Tossan, R. Dixon, J. Power Sources 206 (2012) 349–356.
[24] L. Saw, K. Somasundaram, Y. Ye, T. Tay, J. Power Sources 249 (2014) 231–238.
[25] X. Liu, Z. Chen, C. Zhang, J. Wu, Appl. Energy 123 (2014) 263–272.
[26] J. Yi, U. Kim, C. Shin, T. Han, S. Park, J. Power Sources 244 (2013) 143–148.
[27] X. Rui, Y. Jin, X. Feng, L. Zhang, C. Chen, J. Power Sources 196 (2011) 2109–2114.
[28] Y. Xing, W. He, M. Pecht, K. Tsui, Appl. Energy 113 (2014) 106–115.
[29] J. Kim, B. Cho, IEEE Trans. Energy Convers. 28 (2013) 1–11.
[30] K. Mamadou, E. Lemaire, A. Delaille, D. Riu, S. Hing, Y. Bultel, J. Electrochem. Soc. 159 (2012) A1298–A1307.
[31] T. Dong, M. Montaru, A. Kirchev, M. Perrin, F. Lambert, Y. Bultel, ECS Trans. 35 (2012) 229–237.
[32] QC/T 897-2011, Technical Specification of Battery Management System for Electric Vehicles, 2011.